International Journal of Biological Macromolecules 190 (2021) 607–617

Contents lists available at ScienceDirect

International Journal of Biological Macromolecules

journal homepage: www.elsevier.com/locate/ijbiomac

Silk sericin application increases bone morphogenic protein-2/4 expression via a toll-like receptor-mediated pathway

You-Young Jo [a,1], HaeYong Kweon [a], Dae-Won Kim [b,1], Kyunghwa Baek [c], Weon-Sik Chae [d], Yei-Jin Kang [e], Ji-Hyeon Oh [e], Seong-Gon Kim [e,*], Umberto Garagiola [f]

[a] Sericultural and Apicultural Materials Division, National Institute of Agricultural Sciences, RDA, Wanju 55365, Republic of Korea
[b] Department of Oral Biochemistry, College of Dentistry, Gangneung-Wonju National University, Gangneung 28644, Republic of Korea
[c] Department of Pharmacology, College of Dentistry and Research Institute of Oral Science, Gangneung-Wonju National University, Gangneung 28644, Gangwondo, Republic of Korea
[d] Daegu Center, Korea Basic Science Institute, Daegu 41566, Republic of Korea
[e] Department of Oral and Maxillofacial Surgery, College of Dentistry, Gangneung-Wonju National University, Gangneung 28644, Republic of Korea
[f] Biomedical, Surgical and Oral Sciences Department, Maxillofacial and Dental Unit, School of Dentistry, University of Milan, Milan, Italy

ARTICLE INFO

Keywords:
Silk sericin
Bone morphogenic protein
Osteogenesis

ABSTRACT

Bone morphogenic protein-2/4 (BMP-2/4) is an osteoinductive protein that accelerates osteogenesis when administered to bony defects. Sericin is produced by silkworms, and has a biological activity that differs depending on the degumming method used. Our results indicated that the high molecular weight fraction of silk sericin (MW > 30 kDa) obtained via sonication had a more abundant β-sheet structure than the low molecular weight fraction. Administration of the β-sheet structure silk sericin increased BMP-2/4 expression in a dose-dependent manner in RAW264.7 cells and human monocytes. This sericin increased the expression levels of toll-like receptor (TLR)-2, TLR-3, and TLR-4 in RAW264.7 cells. Application of a TLR-2 antibody or TLR pathway blocker decreased BMP-2/4 expression following sericin administration. In the animal model, the bone volume and BMP-2/4 expression were higher in rats treated with a sericin-incorporated gelatin sponge than in rats treated with a gelatin sponge alone or a sponge-incorporated with denatured sericin. In conclusion, sericin with a more abundant β-sheet structure increased BMP-2/4 expression and bone formation better than sericin with a less abundant β-sheet structure.

1. Introduction

Biomaterial implants are foreign materials that are grafted into the body. Accordingly, host immune responses typically follow grafting. The host immune response against grafts can have either detrimental or beneficial effects on wound healing and repair processes [1]. The recent design of biomaterials has shown a paradigm shift from biocompatible to immunomodulatory [2]. In the case of bone repair, a new bone graft should stimulate macrophages and allow them to create an osteogenesis-compatible environment. This property is called "osteoimmunomodulatory property" [1]. Proteins from silkworm cocoons have been used for bone tissue engineering [3–5] and may have osteoimmunomodulatory properties.

Silkworm cocoons are predominantly composed of silk fibroin and silk sericin. Silk fibroin has been studied as a scaffold for tissue engineering [3,4]. Silk sericin is removed by the degumming process in the silk industry and is thus considered an industrial waste product. Recently, silk sericin has been used as a dressing for skin tissue defects and bone tissue engineering [5]. Silk sericin derived from non-mulberry silkworm cocoons promotes the osteogenic differentiation of bone marrow-derived stem cells (BMSCs) [6]. Silk sericin originating from *Bombyx mori* cocoons also shows osteogenic differentiation of BMSCs [7]. Silk sericin is used as a coating material for titanium implants, as it increases osteogenic signals, such as bone sialoprotein, osteocalcin, and alkaline phosphatase (AP) [8]. Sericin-incorporated gels show a higher expression of AP and runt-related transcription factor 2 (Runx2) in

* Corresponding author.
E-mail addresses: yyjo@rda.go.kr (Y.-Y. Jo), hykweon@korea.kr (H. Kweon), kimdw@gwnu.ac.kr (D.-W. Kim), kb2012@gwnu.ac.kr (K. Baek), wschae@kbsi.re.kr (W.-S. Chae), kyj292@hanmail.net (Y.-J. Kang), oms@gwnu.ac.kr (J.-H. Oh), kimsg@gwnu.ac.kr (S.-G. Kim), umberto.garagiola@unimi.it (U. Garagiola).
[1] Both authors contributed equally to this work.

https://doi.org/10.1016/j.ijbiomac.2021.09.021
Received 14 July 2021; Received in revised form 30 August 2021; Accepted 5 September 2021
Available online 9 September 2021

mesenchymal stem cells [9]. As silk sericin is a protein, its conformation and biological properties differ based on degumming [10] and sterilization processes [11].

Silk mat is a product of silkworm cocoons and is produced by a simple separation method [12]. Silk sericin is the main protein released from the silk mat when the silk mat is placed into a saline solution [13]. The silk sericin is found in a fragmented form [13]. As silk mats contain many trace components, such as protease inhibitors and seroin, these proteins can be found in the saline solution brewed from the silk mat [14]. The composition of these proteins in the solution may differ depending on the silkworm species [10]. In the case of a flatwise-spun silk mat, the content of sericin and trace components is approximately 40% [15]. The application of the silk mat as a membrane for guided bone regeneration has been successful in both preclinical [16] and clinical trials [17]. The mechanism of silk mat-derived bone formation has been partially explained by the tumor necrosis factor-alpha (TNF-α)-mediated pathway [16]. However, the association between TNF-α levels and new bone formation remains controversial. When silk mat-brewed normal saline was administered to RAW264.7 cells, the bone morphogenic protein-2 (BMP-2) mRNA expression level was increased [18]. Considering previous studies [9], silk sericin may be an inducer of BMP-2 in RAW264.7 cells. However, this hypothesis needs to be confirmed.

Proteins in the BMP family are known to promote inductive bone regeneration [19]. Among these, BMP-2 has been widely used clinically [20,21]. The most common complication of recombinant human BMP-2 (rhBMP-2) is acute swelling and pain in the early phase of follow-up [22]. As rhBMP-2-associated complications usually subside within a week postoperatively, these complications are considered a transient reaction. An additional disadvantage of rhBMP-2 usage is its potential role in carcinogenesis [23]. Considering the early and extensive loss of applied rhBMP-2 at the graft site, a relatively high dose of rhBMP-2 should be applied for bone regeneration, which increases the risk of carcinogenesis [24]. In addition, postoperative swelling after the application of rhBMP-2 is dose-dependent [25]. Accordingly, direct application of a high dosage of rhBMP-2 may not be recommended, and sustained release from a proper drug carrier is needed [26,27]. If an unidentified protein from a silk mat can induce BMP-2 in macrophages, the application of a silk mat can serve as an indirect application of rhBMP-2 and is considered a physiological expression. Furthermore, the isolation of a BMP-2 inducer from a silk mat may be applied in bone tissue engineering.

The objectives of this study were as follows: (1) identification of BMP-2 inducers among proteins in the silk mat, and (2) identification of the BMP-2-inducing mechanism by silk proteins. To achieve the first objective, the proteins from a silk mat brewed solution were separated by two-dimensional electrophoresis (2DE) and identified using liquid chromatography-tandem mass spectrometry (LC-MS/MS). The protein conformation was examined using Fourier transform infrared spectroscopy (FT-IR) and circular dichroism (CD) spectroscopy. As the protein profile differs depending on the degumming method used, we applied different degumming methods to ensure that the target protein range could be narrowed. As any protein from a silk mat is a foreign protein for mammals, foreign material recognizing receptors such as toll-like receptors (TLRs) are candidate receptors for the BMP-expressing pathway. The effect of macrophage-derived BMP-2 on osteoblast activation was evaluated using a co-culture system. Additionally, the identified BMP-inducer from the silk mat was incorporated into a gelatin sponge and grafted onto a calvarial defect in rats. In this animal study, bone regeneration was compared to that in the control group.

2. Material and methods

2.1. Sericin extraction

In this study, sericin was extracted using three different methods

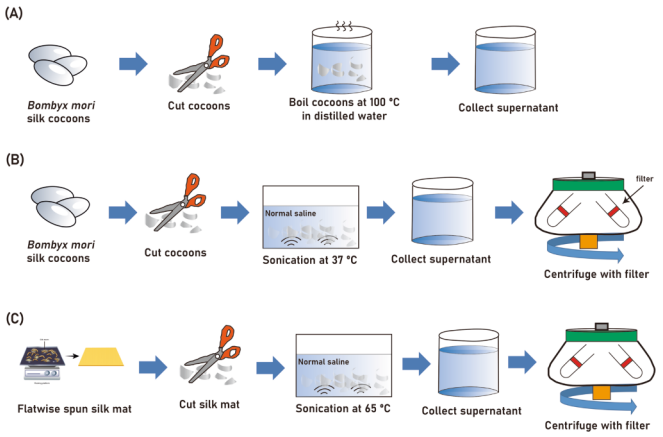

Fig. 1. Sericin preparation methods. (A) Sericin was extracted as a degumming product by boiling silkworm cocoons in distilled water without adding any salt. (B) Silkworm cocoons were sliced and placed into normal saline (37 °C), and sonicated for 48 h. The water-soluble silk protein fraction was separated according to the molecular weight using a filter (Microcon®-30, Merck Millipore Ltd., Tullagreen, Ireland). The filtering procedure was performed in accordance with the manufacturer's protocol. High and low molecular weight fractions were stored separately for further experiments. (C) Flatwise-spun silk mats were sliced. The soluble protein silk fraction from the flatwise-spun silk mat was extracted into normal saline solution via sonication at 65 °C for 2 h. The filtering procedure was the same as above. Only the high molecular fraction was collected.

(Fig. 1). Sericin was extracted as a degumming product by boiling silkworm cocoons in distilled water without adding any salt. Silkworm cocoons and flatwise-spun silk mats were obtained from the same species, *Bombyx mori*. The water-soluble silk protein fraction was extracted by sonication of the silkworm cocoons in warm saline solution (37 °C). The sericin content in silkworms is approximately 20%; however, the content in flatwise-spun silk mats is approximately 40% [15]. The soluble silk protein fraction from the flatwise-spun silk mat was extracted by placement into a normal saline solution, and sonication at 65 °C. The extracted silk protein was separated using Microcon®-30 filter (Merck Millipore Ltd., Tullagreen, Ireland). Filtering was performed according to the manufacturer's protocol.

For a comparison of biological performance, sericin from *B. mori* was purchased from Sigma Aldrich (CAT#: S5201, St. Louis, MO, USA). For a comparison of the protein conformation with different degumming methods, silk sericin extracted from 8 M urea was provided by the Rural Development Administration (RDA, Wanju, Korea).

2.2. 2DE

The protein samples were sent to ProteomeTech Inc. (Seoul, Korea) for analysis. Subsequent 2DE and LC-MS/MS were performed at ProteomeTech Inc. (Seoul, Korea). Briefly, the protein samples were suspended in the prepared solution. The solution was prepared as per the manufacture's protocol. After determining the protein concentration, the protein lysates (600 μg) were loaded onto rehydrated immobilized pH gradient strips using an IPGphor III (GE Healthcare Life Sciences, Pittsburgh, PA, USA), and two-dimensional separation was performed. The gels were fixed for 1 h in a solution of 40% (*v*/v) methanol containing 5% (v/v) phosphoric acid, after which the gels were stained with colloidal Coomassie blue G-250 solution (ProteomeTech). After washing with deionized water, images were acquired using an image scanner (Bio-Rad, Hercules, CA, USA). Selected protein bands were excised from the stained gels and cut into pieces. Proteins were extracted from the excised gels and cut using trypsin. Tryptic peptides were extracted and concentrated using a centrifugal vacuum concentrator. Prior to mass spectrometric analysis, the peptide solution was subjected to a desalting

process using a reversed-phase column [28].

2.3. Identification of proteins via LC-MS/MS

LC–MS/MS analysis was performed using a nano ACQUITY UPLC and LTQ-orbitrap-mass spectrometer (Thermo Electron, San Jose, CA, USA). For tandem mass spectrometry, mass spectra were acquired using data-dependent acquisition with a full mass scan (300–2000 m/z), followed by MS/MS scans. The individual MS/MS spectra were processed using SEQUEST software (Thermo Quest, San Jose, CA, USA), and the generated peak lists were used to query the in-house database using the Mascot program (Matrix Science Ltd., London, UK). The MS/MS ion mass tolerance was 0.8 Da, and the allowance of missed cleavage was 1. The charge states (+2, +3) were considered in the data analysis. The identified protein list showed only significant hits, as defined by Mascot probability analysis.

2.4. Analysis of protein conformation based on FT-IR spectroscopy and CD spectra

FT-IR absorption spectra were measured for the as-dried samples using a Fourier-transform IR spectrometer (Vertex 80, Bruker Optics) equipped with an attenuated total reflectance (ATR) accessory (MIRacle, PIKE technologies) and a mercury cadmium telluride detector. For comparative purposes, sericin extracted with 8 M urea was also used. The absorbance of the freeze-dried sericin specimens was measured at 400–4000 cm^{-1}. The resolution was 4 cm^{-1}, and the average spectra were acquired using 32 repeats. The observed peak of sericin at 1620 cm^{-1} corresponds to the amide I peak. After confirmation of the amide I peak, the amide I crystallinity index (%) was calculated using the following equation:

$$\text{Amide I crystallinity index } (\%) = \frac{A_{1620cm^{-1}}}{A_{1645cm^{-1}} + A_{1620cm^{-1}}} \times 100\ (\%)$$

where $A_{1620cm\text{-}1}$ and $A_{1645cm\text{-}1}$ are the absorbances at 1620 cm^{-1} and 1645 cm^{-1}, respectively.

CD spectra were measured using a CD spectrometer (J-1500, Jasco, Tokyo, Japan). The specimen was solubilized in triple-distilled water and the final concentration was set as 0.02 mg/mL. The solution was placed into a 1 cm cuvette and equipped to the machine. Scanning was performed at 190–260 nm and 20 °C, and the average spectrum was acquired based on three repeats. The graph was smoothed using the Savitzky-Golay algorithm. The baseline was the CD spectrum of triple-distilled water. Conformation analysis was performed using the software provided by the manufacturer.

2.5. Silk sericin release from gelatin sponges

After absorption of sericin, the gelatin sponge (approximate weight: 17.8 mg) was placed into a 24-well culture plate. Each piece of sponge was released in 1 mL of 0.01 M PBS at 37 °C. At predetermined times (8, 24, 48, 72, 120, and 168 h), the PBS was removed and frozen at −20 °C before subsequent analysis, and 1 mL of fresh PBS was added to continue protein release. The protein release solutions were monitored using a spectrophotometer. As gelatin sponge could degrade in PBS, gelatin sponge without sericin was also placed into 24-wells. The fluorescence peak height was correlated with the standards of known sericin concentrations. The protein degraded by the gelatin sponge was subtracted from the measured concentration. The corrected value was used to determine the sericin concentrations in the sponge release samples. Measurements were repeated five times.

2.6. Cell cultures and sericin treatment

RAW264.7 murine macrophages (Korean Cell Line Bank No. 40071), THP-1 human monocytes (Korean Cell Line Bank No. 40202), and U-937 human monocyte-like cells (Korean Cell Line Bank No. 21593.1) were suspended in culture medium. Cells were placed in 6-well culture plates and treated with 1, 5, and 10 μg/mL of either degumming product or separated soluble silk protein fraction. After 2, 8, and 24 h of culture, the cells were collected. Cells in the control culture were treated with a volume of solvent equivalent to that required for sericin.

RAW264.7 cells were pretreated with neutralizing antibodies against mTLR-2 (dilution ratio = 1: 500). Thereafter, 1, 5, and 10 μg/mL of the separated soluble silk protein fraction were applied. The change in BMP-2/4 expression level was evaluated 24 h after sericin administration and compared to that of the cells without the neutralizing antibodies. Toll/interleukin-1 receptor-domain-containing adapter-inducing interferon-β (TRIF) and myeloid differentiation primary response 88 (MyD88) are downstream signal transducers for TLRs. The inhibitory peptides for TRIF and MyD88 were purchased from Sigma-Aldrich. After pretreatment with the inhibitory peptides for TRIF or MyD88; 1, 5, and 10 μg/mL of separated soluble silk protein fractions were applied. The change in BMP-2/4 expression level was evaluated 24 h after sericin administration and compared to that of the cells without the inhibitory peptides.

To confirm the immunomodulatory effect of sericin administration, RAW264.7 cells were co-cultured with MC3T3-E1 cells (mouse osteoblasts). Cells were cultured at confluence, and the inserts containing RAW264.7 cells were combined with MC3T3-E1 cells. Once the inserts were placed in the wells, all cells were treated with a differentiation medium, namely, BGJb medium (Life Technologies, Carlsbad, CA, USA) supplemented with 1% fetal bovine serum, 100 IU/mL penicillin, 100 IU/mL streptomycin, 100 μg/mL ascorbic acid, and 0.3 mM Na_3PO_4, pH 7.4. The treated concentration of sericin was 1 μg/mL and 10 μg/mL. To exclude the effect from solvent for sericin (normal saline), normal saline without sericin was also applied. Accordingly, there were 4 groups (untreated control, solvent only, 1 μg/mL sericin, and 10 μg/mL sericin). The medium was changed every other day until the harvest. All experiments were performed at least in triplicates.

2.7. Quantitative reverse transcriptase-polymerase chain reaction (qRT-PCR) and Western blotting

To analyze the expression of BMP-2/4 induced by each sericin, we treated the cells with 1, 5, and 10 μg/mL of sericin. To assess the relative mRNA expression level of BMP-2 compared to GAPDH, total RNA was extracted from the cells. The detailed procedure for qRT-PCR was described in our previous publication [29]. The primers used are listed in Supplementary Table 1.

Proteins were collected and mixed with a sodium dodecyl sulfate buffer. After heat denaturation, the proteins were electrophoresed on a 10% polyacrylamide gel. The gels were then transferred onto polyvinylidene difluoride membranes. After blocking, the membranes were probed with primary antibodies (1:500 dilution). The sources and specifications of primary antibodies were as follows: BMP-2/4 (Santa Cruz Biotech), Runx2 (Santa Cruz Biotech), alkaline phosphatase (Santa Cruz Biotech), osteocalcin (Santa Cruz Biotech), osteopontin (Santa Cruz Biotech), TLR-2 (Abcam), TLR-3 (Abcam), TLR-4 (Abcam), and TLR-7 (Abcam). Blots were imaged and quantified using a ChemiDoc XRS system (Bio-Rad Laboratories).

2.8. Animals and experimental design

Eight-week-old Crl:CD (Sprague-Dawley) specific pathogen-free (SPF)/VAF outbred rats (Orientbio Inc., Sungnam, Korea) were used in this study. All procedures were performed in accordance with the guidelines for laboratory animal care and were approved by the Gangneung-Wonju National University for Animal Research (GWNU-2018-14). Twenty-seven rats (2–3 rats per cage) were housed under a 12-h light/12-h dark cycle in a controlled environment at 20–22 °C and 40% humidity for one week for acclimation prior to experimentation.

The rats had free access to food and water and were all fed a controlled semisynthetic diet according to a classical recommendation (74% carbohydrates from soybean vegetable oil, 14% protein from casein, supplemented with a standard vitamin and mineral mix).

The rats were divided into four groups. Considering the high mortality rate in critical-sized calvarial defect surgery, additional animals were assigned to each group. Graft materials comprised a gelatin sponge (Cutanplast Dental®, Uniplex, Sheffield, UK), gelatin sponge (Cutanplast Dental®) with sericin, and gelatin sponge (Cutanplast Dental®) with heat-denatured sericin. The amount of sericin in each graft was approximately 50 μg. Group U, composed of six individuals, underwent anesthesia and an incision, but received no graft. Animals in group G (six individuals) were treated with a gelatin sponge, and the animals in group G + S (ten individuals) were treated with a gelatin sponge containing sericin. Group G + D animals (five individuals) were treated with a gelatin sponge containing denatured sericin. The anesthetic solution was a combination of 0.5 mL Zoletil (125 mg/mL; Bayer Korea, Seoul, Korea) and 0.5 mL of Xylazine (Rompun; Bayer Korea). The injected amount was 0.3 mL for each rat. After sterilization of the skin, a mid-sagittal incision was made on the calvaria. A critical-sized defect was prepared in the calvaria using a trephine bur (diameter: 8.0 mm). After placing the graft, the skin and periosteum were sutured simultaneously using 3–0 black silk. Antibiotics (gentamicin; Daesung, Yiwang, Korea) and analgesics (tolfenamic acid; Samyang anipharm, Seoul, Korea) were administered postoperatively. The dosages of gentamicin and tofenamic acid were 5 and 4 mg/day, respectively. Drugs were administered for 48 h postoperatively. In the first 24 h, one animal from group G and two animals from group G + S died. Accordingly, six animals from group U, five from group G, eight from group G + S, and five from group G + D were observed until 8 weeks postoperatively. After 8 weeks, all rats were sacrificed, and specimens from the calvaria were processed for further analysis.

2.9. Micro-computerized tomography (mCT)

The calvarial specimens (10 × 10 × 0.5 mm) were sent to Genoss (Sungnam, Korea) for mCT analysis. The procedure was performed according to the method described in our previous publications [10,14]. Briefly, the SkyScan1173 system (Skyscan, Kontich, Belgium) was used for the analysis. The source voltage was set to 90 kVp. An aluminum filter was used, and the image pixel size was 9.04 μm. The scanned images were reconstructed using Nrecon software (V.1.7.0.4, Micro Photonics Inc., Allentown, PA, USA). Additional images were obtained using μCT50 (Scanco Medical, Brüttisellen, Switzerland) at the Center for Scientific Instruments, Gangneung-Wonju National University (Gangneung, Korea) for repeated checking. The size of the initial surgical defect was referenced to determine the region of interest (ROI). The bone volume (BV) in the ROI was analyzed using mCT software (CT Analyzer V.1.17.7.2+, Skyscan). The images were analyzed with a lower grayscale threshold and an upper grayscale threshold set to 48 and 255, respectively.

2.10. Immunohistochemical determination and western blot analysis in tissue samples

Fresh calvarial tissues were fixed with 4% paraformaldehyde at 4 °C for 8 h. After washing the fixed samples with tap water, the samples were placed in a decalcification solution (CAT#: MKCL9701, Sigma-Aldrich). The samples were then placed on a rocking plate for 3–5 d. Decalcification was evaluated using a microtome blade. The decalcified tissues were placed in a tissue processer and embedded into paraffin. To assess the expression of BMP-2/4, we performed immunohistochemical staining using anti-BMP-2/4 antibodies (CAT#: sc-137087, Santa Cruz Biotech). Immunohistochemical analysis was performed according to the procedure reported in our previous publication [16]. Briefly, sections were prepared, and enzyme predigestion was performed using a proteolytic enzyme (1 mg porcine trypsin, Sigma-Aldrich). The sections were then treated with hydrogen peroxide. After washing and blocking, the sections were treated with primary antibodies (BMP-2/4, dilution ratio = 1:100). After conjugation with a universal secondary antibody (Dako REAL™ EnVision™/HRP, Rabbit/Mouse; Dako North America Inc.), the slides were stained with a mixture of diaminobenzidine chromogen and hydrogen peroxidase (Dako REAL™ DAB+ Chromogen and Dako REAL™ Substrate Buffer; Dako North America Inc.).

Protein extraction from tissue was performed using a commercially available kit (CAT#: ab270054, Abcam). After weighing out the tissue, protein extraction buffer was prepared at a ratio of 10 mL buffer per 1 g of tissue. After adding protease inhibitors to the protein extraction buffer, the tissue samples were homogenized with the buffer. The protein was denatured for 5 min and then cooled at 4 °C for 1 h. The mixtures were centrifuged at 15000 ×*g* for 10 min. After determining the concentration of extracted proteins, the specimen was loaded onto the gel, and the subsequent procedure was performed as described above.

2.11. Statistical analysis

All cellular experiments were performed in triplicates in this study. Data are reported as the mean ± standard deviation. One-way analysis of variance was used for comparison among groups. For the post-hoc test, the Bonferroni test was used. The significance level was set as at $P < 0.05$.

3. Results

3.1. High molecular weight sericin fraction (>30 kDa) extracted via sonication at 37 °C and 65 °C showed higher BMP-2/4 expression

Proteins extracted by boiling in distilled water showed a dragged band around pI 3 and no other prominent protein spots (Fig. 2A). The excised band was identified as fragmented sericin 1. In comparison, the soluble fractions extracted by sonication at 37 °C showed a greater number of protein spots (Fig. 2B). Eight spots were selected, as shown in Fig. 2B, and respective the results are listed in Supplementary Table 2. When the temperature was increased to 65 °C, many of these protein spots disappeared (Fig. 2C). Accordingly, two spots were selected; spot 1 in Fig. 2C was identified as a mixture of sericin 1 and sericin 3, and spot 2 (Fig. 2C) was identified as sericin 3. Both spots were fragmented, considering their original molecular weights. Purchased sericin had a similar isoelectric point compared to the sericin extracted by boiling distilled water, but had different molecular weight fractions (Fig. 2D).

The extracted protein fraction was applied to RAW264.7, and the ability of the protein to increase BMP-2/4 expression was examined. The protein from the degummed product showed a very weak increase in BMP-2/4 (Fig. 2E). When sonication products were separated by their molecular weight, the fraction with a higher molecular weight (>30 kDa) showed a higher level of BMP-2/4 increase when compared to the fraction with a lower molecular weight (<30 kDa) (Fig. 2F). The protein fraction from flatwise-spun silk (molecular weight >30 kDa) also showed increased levels of BMP-2/4 expression (Fig. 2G). Purchased sericin did not induce BMP-2/4 expression in RAW264.7 cells (Fig. 2H). Similarly, the BMP-2 mRNA expression levels were not significantly increased by the sericin extracted in boiling distilled water (Fig. 2I) or sericin from the low molecular weight fraction (Fig. 2J). BMP-2 mRNA expression levels were significantly increased by sericin from the high molecular weight fraction compared to the untreated control ($P < 0.05$) (Fig. 2K). When sericin from the high molecular weight fraction was administered to THP-1 and U-937 cells, the BMP-2/4 expression level also increased (Fig. 2L).

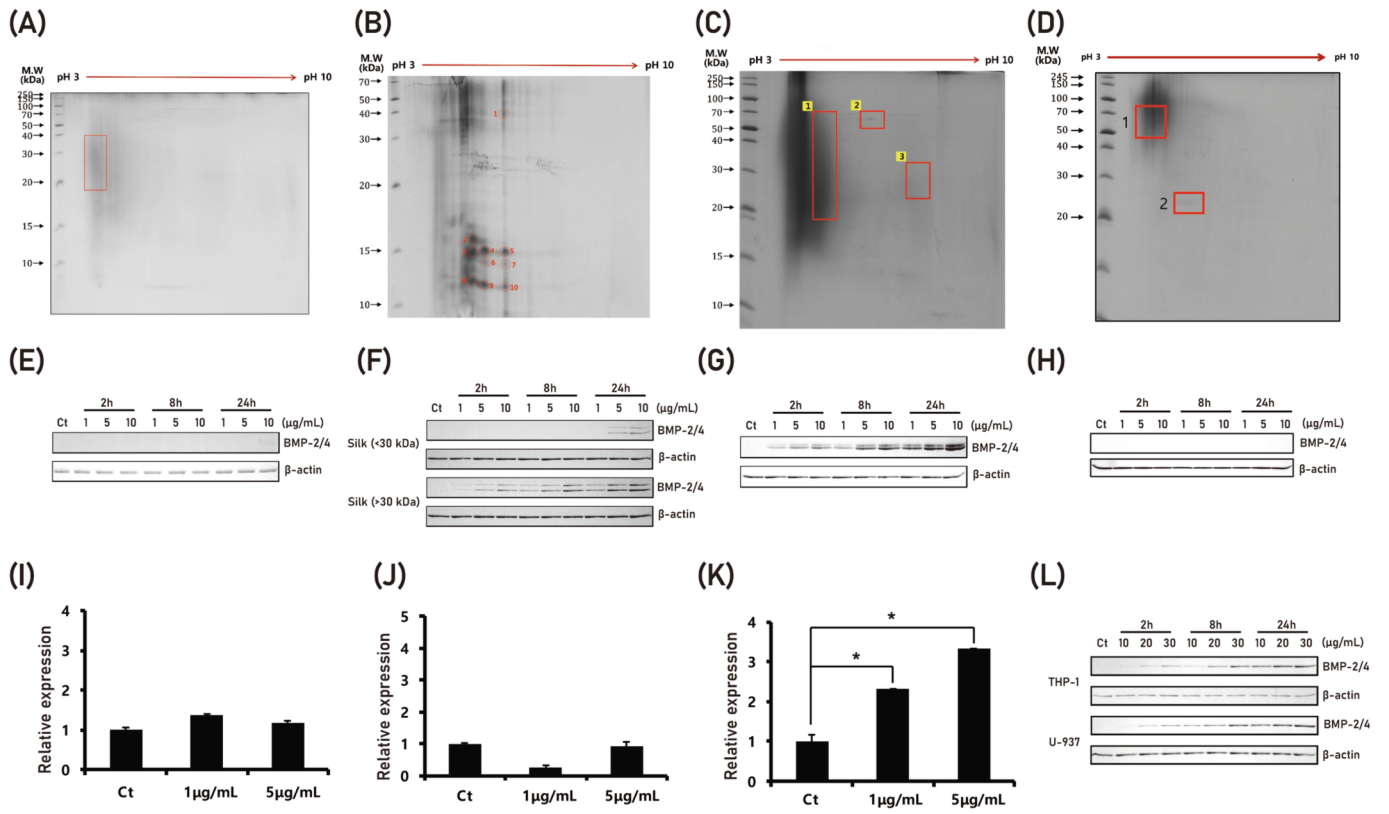

Fig. 2. BMP-2/4 induction by different types of extracted silk protein. The results of 2D electrophoresis demonstrated that the separated protein profiles differed depending on the degumming method used. (A) The samples extracted using boiling distilled water contained few proteins. The red angled portion was excised and identified as sericin 1. (B) Many protein spots were identified in the solution extracted using normal saline via sonication at 37 °C. Detailed protein profiles are presented in Supplementary Table 2. (C) The number of protein spots decreased at elevated temperature. Spot 1 was identified as a mixture of sericin 1 and sericin 3. Spot 2 was sericin 3. (D) The isoelectric point of purchased silk sericin was similar to that in (A), but had a different molecular weight fraction. Two spots were identified as silk sericin. When silk sericin from (A) was added to RAW264.7 cells, BMP-2/4 expression was barely visible (E). However, the high molecular fractions of (B) and (C) showed strong BMP-2/4 expression ((F) and (G), respectively). Similar to the silk sericin in (A), the purchased silk sericin showed poor BMP-2/4 induction (H). BMP-2 mRNA was also consistent with the protein expression level. Silk sericin extracted using boiling distilled water (I) and the low molecular weight fraction from sonication (J) did not show significant difference in BMP-2 mRNA expression compared to the untreated control ($P > 0.05$). However, high molecular weight fraction from sonication (K) showed significant difference in BMP-2 mRNA expression compared to the untreated control ($^*P < 0.05$). The BMP-2/4 induction-ability of the high molecular weight fraction of sericin from sonication was also shown in human monocyte cell lines such as THP-1 and U-937 cells (L). (For interpretation of the references to colour in this figure legend, the reader is referred to the web version of this article.)

3.2. Difference in sericin protein conformation with different degumming methods

The FT-IR absorption spectra of the sericin protein showed distinctive absorptions at 1600–1700 (amide I), 1480–1580 (amide II), and 1230–1300 cm^{-1} (amide III), as shown in Fig. 3A [16,30]. The amide I peak (C═O stretching) was sensitively shifted depending on the protein secondary structure [30]. Thus, careful sub-band analysis of the amide I absorption band can enable the estimation of the relative abundance of protein secondary structures. Compared to the conventional infrared spectra (Fig. 3B), in this study, the second derivative infrared spectra of the silk proteins distinctly showed sub-band absorptions corresponding to the protein secondary structures (Fig. 3C). Both of the examined protein samples were proven to have β-sheets, β-turns, and random structures. The high molecular weight fraction of silk sericin (MW > 30 kDa) obtained by sonication showed enhanced abundance of β-sheet structures (1617, 1625, and 1698 cm^{-1}), whereas the low molecular weight fraction of silk sericin (MW < 30 kDa) showed a relatively enhanced abundance of β-turn (1666, 1675, and 1686 cm^{-1}) and random (1652 cm^{-1}) structures.

The boiling water and urea groups exhibited similar CD spectra (Fig. 3D). Random coils were the dominant structures in both of the groups. However, the GW group showed a strong negative peak at approximately 225 nm representing a β-sheet structure. When the sericin from the GW group was denatured by heating at 100 °C for 10 min, the peak of approximately 225 nm was diminished (Fig. 3E). Interestingly, sericin from the company did not exhibit a peak at 225 nm (Supplementary Fig. 1). Fig. 3F shows the normalized release profiles of gelatin sponges with silk sericin. Approximately 45% of the total sericin was released in the first 8 h. Thereafter, 75% of the total sericin was released within 48 h. The released amount was sharply reduced after 72 h and 96% of the total sericin was released before 168 h.

3.3. BMP-2/4 produced by RAW264.7 cells stimulated osteoblasts

RAW264.7 cells were co-cultured with MC3T3-E1 cells for 7 d (Fig. 4A). The application of sericin to RAW264.7 cells increased the expression level of BMP-2/4 (Fig. 4B). To examine the potential activation of osteoblasts by BMP-2/4 from RAW264.7 cells, the expression levels of Runx2, osteopontin, and osteocalcin were evaluated in co-cultured osteoblasts. Compared to the untreated control, osteoblasts co-cultured with sericin-treated RAW264.7 cells exhibited elevated expression levels of Runx2, osteopontin, and osteocalcin (Fig. 4B).

3.4. BMP-2/4 expression after sericin application was mediated by the TLR pathway

The application of sericin extracted by sonication resulted in

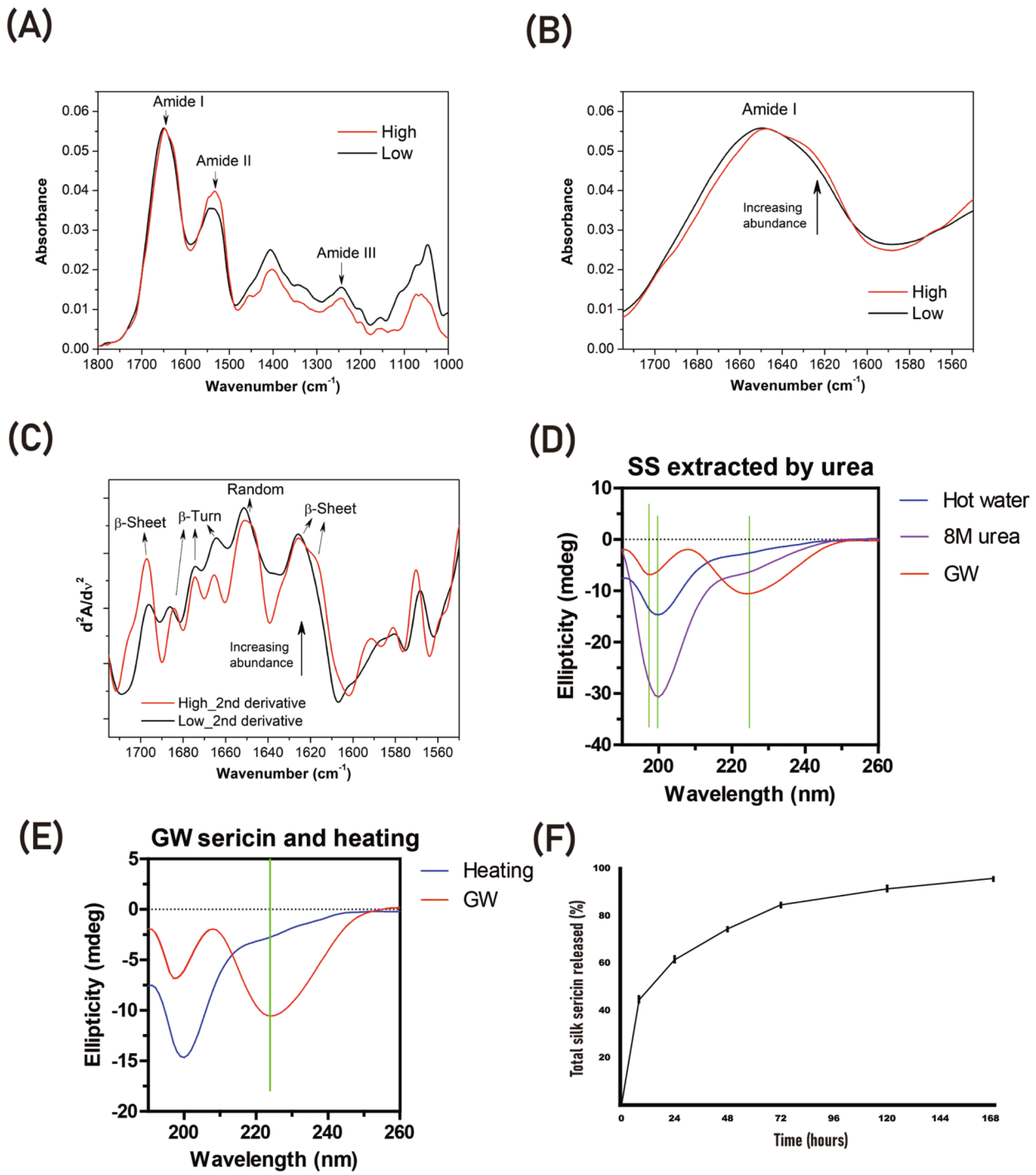

Fig. 3. P Protein conformation of each fraction. (A) ATR-FT-IR spectra of the sericin proteins: high molecular weight fraction (solid) and low molecular weight fraction (dotted). (B) IR absorptions in the amide I region of the sericin proteins: high molecular weight fraction (solid) and low molecular weight fraction (dotted). (C) The second derivative infrared spectra of the corresponding sericin proteins. (D) CD spectra: a peak corresponding to the β-sheet structure appeared around 225 nm and was significantly enhanced in the GW group (high molecular weight fraction of the silk sericin extracted by sonication). The negative peak around 200 nm represents random coil structures. (E) CD spectra after heat denaturation: when the sericin from the GW group was denatured by heating at 100 °C, the peak, corresponding to the β-sheet structure, decreased. (F) Sericin release profile from the gelatin sponge. Sericin was rapidly released until 8 h. Thereafter, there was a continued, slower release until 168 h.

elevated expression levels of TLR-2, -3, -4, and -7 (Fig. 5A). In particular, the elevated expression of TLR-2 and -4 was more prominent than that of TLR-3 and -7. When TLR-2 was neutralized by the application of the TRL-2 antibodies, the elevated BMP-2/4 expression with sericin application was reduced (Fig. 5B). The downstream signal transducers for TLR were TRIF and MyD88. After application of the inhibitory peptide for TRIF and MyD88, the elevated BMP-2/4 expression with sericin application was also reduced (Fig. 5C). The ability of silk sericin to induce BMP-2/4 was diminished by additional heating at 100 °C for 10 min (Fig. 5D).

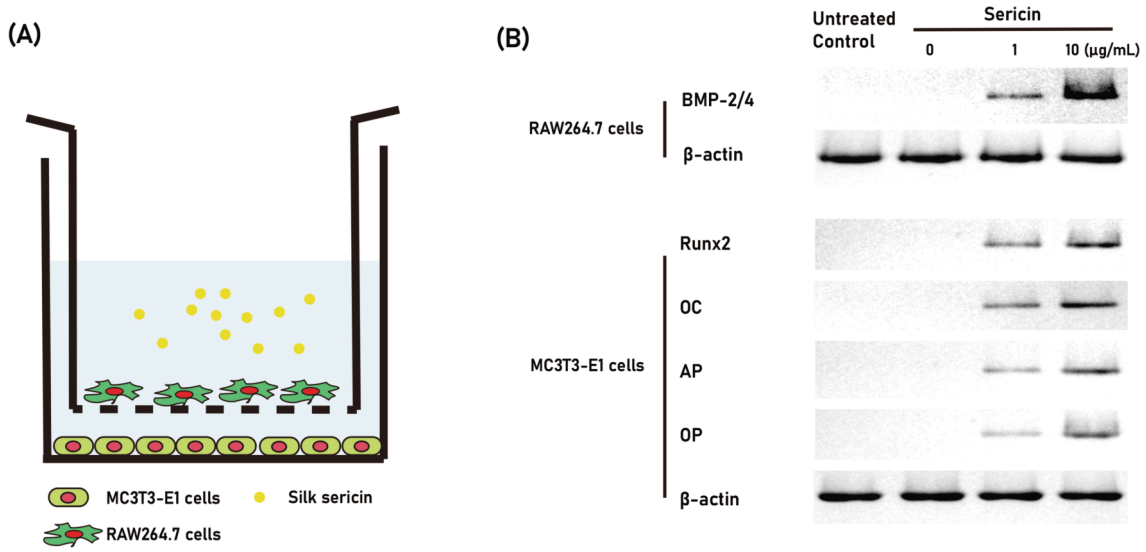

Fig. 4. The results of co-culture with RAW264.7 cells and MC3T3-E1 cells. (A) Schematic drawing of the co-culture system. (B) The application of sericin increased BMP-2/4 levels in the RAW264.7 cells. The expression levels of Runx2, osteocalcin, and osteonectin in MC3T3-E1 cells were higher in the RAW264.7 cells within the sericin application group than those in the RAW264.7 cells without sericin application.

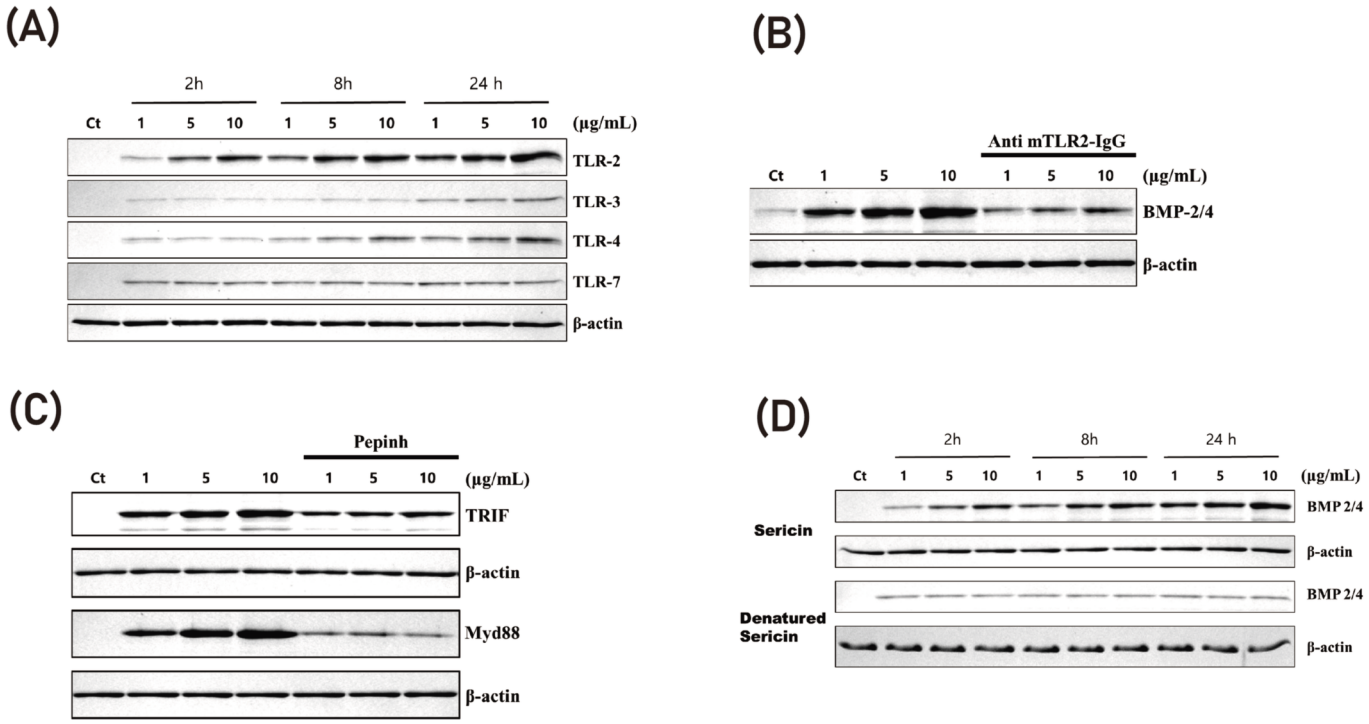

Fig. 5. TLR-mediated pathway activation by sericin. (A) The expression levels of TLR-2, TLR-3, and TLR-4 were increased by sericin application. (B) The application of mouse TLR-2 neutralizing antibodies decreased the BMP-2/4 expression level induced by sericin application. (C) The application of an inhibitory peptide (Pepinh) for TRIF and MyD88 showed a similar effect to application of TLR-2 antibodies. (D) When BMP-2/4–inducing sericin was denatured by heating at 100 °C, the ability of sericin to induce BMP-2/4 expression was decreased in the denatured protein.

3.5. Gelatin sponge incorporated with the high molecular weight (>30 kDa) and abundant β-sheet structured sericin fraction provided better bone regeneration

The gelatin sponge incorporated with the sericin fraction showed higher bone regeneration compared to the unfilled control group, the gelatin sponge-only group, and the group receiving a gelatin sponge with denatured sericin (Fig. 6A). The BV was 0.51 ± 0.40 mm^3 for the unfilled control (U group), 3.13 ± 2.27 mm^3 for gelatin sponge only (G group), 8.48 ± 3.97 mm^3 for gelatin sponge incorporated with sericin (G + S group), and 3.68 ± 1.83 mm^3 for gelatin sponge incorporated with denatured sericin (G + D group) (Fig. 6B). When comparing the BV, the differences among the groups were statistically significant ($P < 0.001$). In the post-hoc test, the difference between G + S group and the other groups was significantly different ($P < 0.001$, =0.015, and = 0.032 for U group, G group, and G + D group, respectively).

The results of immunostaining for BMP-2/4 showed its higher expression in G + S group than in the other groups (Fig. 7A). When the

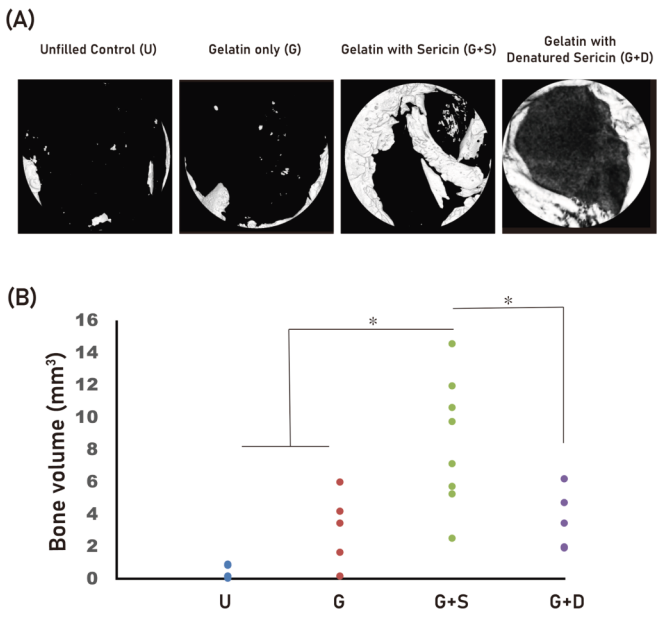

Fig. 6. Results from the micro-computerized tomogram (mCT) analysis. (A) New bone formation was higher in the gelatin + sericin (G + S) group compared to the unfilled control (S), gelatin only (G), and gelatin + denatured sericin (G + D) groups. (B) Comparison of the bone volumes measured via mCT: the G + S group showed a significantly higher value compared to the other groups (*$P < 0.05$).

total tissue proteins were extracted, the expression level of BMP-2/4 was higher in G + S group than in the other groups (Fig. 7B).

4. Discussion

In this study, silk sericin with a more abundant β-sheet structure was found to increase BMP-2/4 expression in RAW264.7 cells (Figs. 2 and 3). Silk sericin extracted in boiling distilled water predominantly exhibited a random coil structure and weakly increased BMP-2/4 expression in RAW264.7 cells (Figs. 2 and 3). The high molecular weight fraction (>30 kDa) extracted at 37 °C increased BMP-2/4 expression in RAW264.7 cells to a much greater extent than the low molecular weight fraction (<30 kDa) under the same conditions (Fig. 2F). The high molecular weight fraction (>30 kDa) extracted at 65 °C from the flatwise-spun silk mat was also identified as sericin and could increase BMP-2/4 expression in RAW264.7 cells (Fig. 2C and G). BMP-2/4 induction after sericin administration was also observed in human monocyte cells such as THP-1 and U-937 cells (Fig. 2L). BMP-2/4 produced by RAW264.7 cells increased the expression levels of Runx2, osteopontin, and osteonectin in co-cultured MC3T3-E1 cells (Fig. 4b). Sericin application increased the expression levels of TLR-2, TLR-3, and TLR-4 (Fig. 5A). The application of either TLR-2 antibodies or inhibitory peptides for TLR downstream signaling decreased BMP-2/4 expression (Fig. 5B and C). When sericin was denatured by heating at 100 °C, the BMP-2/4 induction ability was diminished (Fig. 5D). In the rat calvarial defect model, the group receiving sericin incorporated in a gelatin sponge showed significantly higher BV than the gelatin sponge only group, no graft group, and group receiving a gelatin sponge with denatured sericin ($P < 0.05$; Fig. 6). Collectively, sonication of the silk mat in saline at low temperature (37–65 °C) produced sericin with increased β-sheet conformation (Fig. 3). This sericin increased BMP-2/4 expression levels in macrophages and monocytes via the TLR-mediated pathway (Figs. 2 and 5). As a consequence, gelatin sponges with sericin grafts increased BMP-2/4 expression and BV in critical-sized calvarial defects in rats (Figs. 6 and 7).

Silkworm cocoons are composed of fibrotic and glue-like proteins [3,12], with glue-like proteins connect the fiber and form a firm matrix-like structure. Silk mats are produced from silkworm cocoons via an eco-friendly method [12]. Silk mat application has shown successful bone regeneration using a guided bone regeneration technique [16,17]. When the silk mat is placed in normal saline, the soluble fraction of the glue-like proteins is brewed into saline. When this solution is administered to RAW264.7, elevated expressions of BMP-2 mRNA and BMP-4 mRNA are found in a cDNA microarray assay [18]. Glue-like proteins are composed of different types of proteins [14]. To identify BMP-2/4-inducing proteins among the glue-like proteins, different degumming methods and cellulose filters were used in this study (Fig. 1). Sericin is a glue-like protein making up approximately 20% of the weight fraction of a cocoon [15]. As silk fibroin comprises 75–80% of the weight fraction, sericin is the main glue-like protein of cocoons [15]. In this study, the BMP-2/4-inducing protein was identified as sericin (Fig. 2).

Sericin is made up of a combination of sericin 1 and sericin 3, with heat-extracted sericin having a molecular weight range of 20–200 kDa [31]. Based on the amino acid sequence, sericin 1 has a molecular weight of 119.5 kDa and sericin 3 has a molecular weight of 123.3 kDa [32], whereas most protease inhibitors and seroins have low molecular weights (<30 kDa) [14]. Accordingly, the high molecular weight fraction (>30 kDa) was expected to be a sericin 1/3 mixture. The LC-MS/MS results confirmed this hypothesis (Fig. 2). Administration of this fraction resulted in higher levels of BMP-2/4 expression compared to the other fractions. In the case of the boiled fraction, although the identified protein was sericin 1 only (Fig. 2A), the wide variation in its molecular weight might be due to heat-induced degradation. Flatwise-spun silk mats do not form cocoons, resulting in the lack of an inner layer [15]. In addition, warming saline to 65 °C might accelerate the denaturation of the lower molecular weight protein fraction. As a result, many protein spots observed in the 37 °C extract solution from the silk mat (Fig. 2B) disappeared in the 65 °C extract solution from the flatwise-spun silk (Fig. 2C).

The bone regeneration ability of silk sericin has been widely studied. A high molecular weight fraction of sericin has been used in medical applications [33], and can induce mineralization via hydroxyapatite nucleation [31]. Sericin-incorporated titanium implants increase the mRNA expression of bone sialoprotein, osteocalcin and alkaline phosphatase in osteoblasts [34]. Sericin from *B. mori* induces the nucleation of hydroxyapatite nano-needles [35]. Compared to sericin from *B. mori*, sericin from *Antheraea pernyi* showed higher nucleation of hydroxyapatite crystals [36]. Collagen hydrogel incorporated with silk sericin increases the expression of ALP and Runx2 in mesenchymal stem cells [9]. The biological activity of sericin may differ depending on the extraction conditions. In this study, the high molecular weight sericin fraction with a greater β-sheet structure showed higher expression of BMP-2/4 in RAW264.7 cells (Fig. 2) and BV in rat calvarial bone defects (Fig. 6).

TLRs are pattern-recognizing receptors [37]. When foreign materials are introduced into the body, macrophages recognize them via the TLR [38]. As silk sericin is a foreign protein in mammals, silk sericin is recognized by TLRs in macrophages. Foreign proteins are predominantly recognized by TLR-2 and TLR-4 [39]. In this study, the expression levels of TLR-2, -3, and -4 were increased by sericin administration (Fig. 5A). Many types of inflammation-associated calcifications have been reported [40,41]. Biglycan, a leucine-rich proteoglycan with a β-sheet structure [42], activates TLR-2 and TLR-4 [43,44]. The elevated expression of BMP-2 upon biglycan administration is mediated by TLR-2 [45]. Oxidized low-density lipoprotein (LDL) also induces BMP-2 via the TLR-2/4-mediated pathway [46]. LDL has a 21% β-sheet structure in 0.1 M hydroxyethyl piperazine ethane sulfonic acid at pH 7.4, and 37 °C [47]. Elevated BMP-2 expression is associated with higher levels of TLR-2/4 [48]. TLR-3 activation also induces bone-forming response [49]. In addition to glycoproteins and lipoproteins, other microbial components can also activate TLRs; these TLR-activators increase osteoblast differentiation in a dose- and cellular type-dependent manner [50]. In this study, TLR-2 antibody pre-treatment reduced BMP-2/4 expression

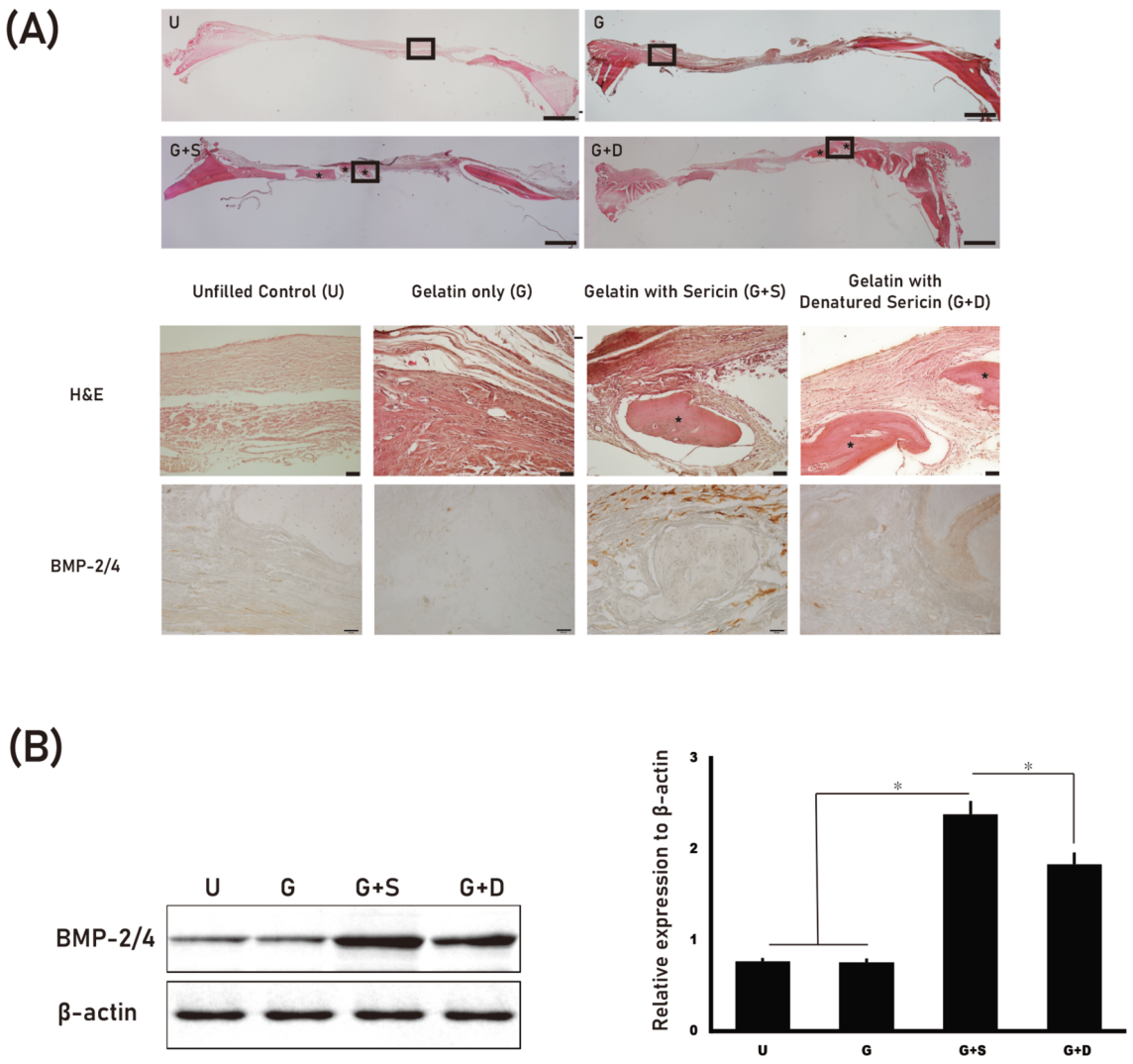

Fig. 7. Results from the histological analysis. (A) New bone formation was increased in the gelatin + sericin (G + S) group, as seen in hematoxylin & eosin (H&E) stain results, compared to the unfilled control (S), gelatin only (G), and gelatin + denatured sericin (G + D) groups. Low magnification view for each group was shown in the upper row. Scale bar represented 1 mm. Zoomed area acquired at 200×. Scale bar represented 50 μm. Bony islands (*) were observed in G + S group and G + D group. The expression level of BMP-2/4 was also higher in the G + S group. (B) Western blots of tissue samples. The G + S group showed a significantly higher value compared to the other groups (*P < 0.05).

following sericin application (Fig. 5B). TRIF and MyD88 are the main downstream signaling proteins involved in the TLR pathway [51]. In this study, the application of their inhibitory peptides also decreased BMP-2/4 expression with sericin application (Fig. 5C). Interestingly, artificial proteins with a cross-β-sheet quaternary structure 2 can activate TLRs for a longer duration and are helpful for the immunization process [52]. Heat denaturation of sericin diminished its β-sheet structure (Fig. 3E), and the application of heat-denatured sericin to RAW264.7 cells produced lower BMP-2/4 expression levels compared to undenatured sericin (Fig. 5D). Amyloid has a cross-β-sheet quaternary structure, and the destruction of this structure abolishes TLR-2 activation by amyloid application [53]. Osteogenesis is further enhanced by M1 macrophages than by M2 macrophages [54]. Sericin is an M1-type macrophage polarizing agent [55], and BMP-2 is secreted by M1 macrophages [56].

Macrophages are important orchestrators for bone regeneration [54], and BMP-2/4 originated macrophages may differentiate mesenchymal stem cells from bone defects as active osteoblasts [54,56]. In this study, the application of sericin to RAW264.7 cells increased the expression level of BMP-2/4 and the expression levels of Runx2, osteopontin, and osteocalcin in co-cultured MC3T3-E1 cells (Fig. 4B). In addition, gelatin sponge-incorporated sericin showed higher bone formation and BMP-2/4 expression levels in rat calvarial defect model (Figs. 6 and 7). When heat-denatured sericin was incorporated, the BV and BMP-2/4 expression levels were decreased compared to their expression levels upon undenatured sericin incorporation (Figs. 6 and 7). The sericin extraction technique used influences the biological activities of sericin [57]. In addition to the extraction technique introduced in this study, many other extraction techniques can be used to produce silk sericin with an abundant β-sheet conformation. Degumming with glycerol supplements increases the β-sheet conformation of silk sericin [58], with glycerol-preserved bone grafts showing clinical performance similar to that of freeze-dried grafts [59]. Therefore, it is evident that there are other efficient techniques available than the technique proposed in this study.

5. Conclusion

In this study, both molecular weight and protein conformation were found to be important for sericin-mediated bone formation. The different degumming methods showed differences in the sericin conformation and molecular weight spectra. Among them, sericin, which has a more abundant β-sheet structure with a high molecular

weight, showed increased osteogenic activity. This sericin increased BMP-2/4 expression levels in macrophages and monocytes via a TLR-mediated pathway.

CRediT authorship contribution statement

Conceptualization, K.D.W., J.Y.Y., and K.S.G.; methodology, K.D.W., J.Y.Y., K.H.Y., and C.W.S.; validation, K.D.W., C.W.S., K.Y.J., and O.J. H.; formal analysis, K.H.Y.; investigation, K.D.W. and B.K.; data curation, C.W.S. and K.S.G.; writing-original draft preparation, K.S.G.; writing-review and editing, C.W.S., U.G., and K.S.G.; supervision, U.G. and K.H.Y.; funding acquisition, K.S.G. and J.Y.Y. All authors have read and agreed to the published version of the manuscript.

Declaration of competing interest

The authors declare that they have no competing interests, as defined by International Journal of Biological Macromolecules, or other interests that might be perceived to influence the results and/or discussion reported in this paper.

Acknowledgments

This study was mainly carried out with the support of “Cooperative Research Program for Agriculture Science and Technology Development (Project no. PJ01562601)” Rural Development Administration, Republic of Korea. Additionally, support was received from the “Research Program for Agricultural Science & Technology Development” (PJ012626022019), National Institute of Agricultural Science, Rural Development Administration, Republic of Korea.

Data availability statement

All datasets used in this study are provided as supplementary data.

Ethical approval and informed consent

The animal experiments in this study were approved by the Gangneung-Wonju National University for animal research (GWNU-2018-14). All animal experiments were performed in accordance with the relevant guidelines and regulations.

Third party rights

The images, drawings, and photographs in this study were taken or created by the authors of the paper.

Appendix A. Supplementary data

Supplementary data to this article can be found online at https://doi.org/10.1016/j.ijbiomac.2021.09.021.

References

[1] Z. Chen, X. Mao, L. Tan, T. Friis, C. Wu, R. Crawford, et al., Osteoimmunomodulatory properties of magnesium scaffolds coated with ß-tricalcium phosphate, Biomaterials 35 (2014) 8553–8565, https://doi.org/10.1016/j.biomaterials.2014.06.038.
[2] S. Franz, S. Rammelt, D. Scharnweber, J.C. Simon, Immune responses to implants - a review of the implications for the design of immunomodulatory biomaterials, Biomaterials 32 (2011) 6692–6709, https://doi.org/10.1016/j.biomaterials.2011.05.078.
[3] J.Y. Song, S.G. Kim, J.W. Lee, W.S. Chae, H. Kweon, Y.Y. Jo, et al., Accelerated healing with the use of a silk fibroin membrane for the guided bone regeneration technique, Oral Surg. Oral Med. Oral Pathol. Oral Radiol. Endod. 112 (2011) e26–e33, https://doi.org/10.1016/j.tripleo.2011.05.002.
[4] S.W. Lee, S.G. Kim, J.Y. Song, H. Kweon, Y.Y. Jo, K.G. Lee, et al., Silk fibroin and 4-hexylresorcinol incorporation membrane for guided bone regeneration, J. Craniofac. Surg. 24 (2013) 1927–1930, https://doi.org/10.1097/SCS.0b013e3182a3050c.
[5] F. Ahsan, T.M. Ansari, S. Usmani, P. Bagga, An insight on silk protein sericin: from processing to biomedical application, Drug Res. (Stuttg) 68 (2018) 317–327, https://doi.org/10.1055/s-0043-121464.
[6] Z. Jiayao, Z. Guanshan, Z. Jinchi, C. Yuyin, Z. Yongqiang, Antheraea pernyi silk sericin mediating biomimetic nucleation and growth of hydroxylapatite crystals promoting bone matrix formation, Microsc. Res. Tech. 80 (2017) 305–311, https://doi.org/10.1002/jemt.22793.
[7] M. Yang, G. Zhou, Y. Shuai, J. Wang, L. Zhu, C. Mao, Ca(2)-induced self-assembly of Bombyx mori silk sericin into a nanofibrous network-like protein matrix for directing controlled nucleation of hydroxylapatite nano-needles, J. Mater. Chem. B 3 (2015) 2455–2462, https://doi.org/10.1039/C4TB01944J.
[8] S. Nayak, T. Dey, D. Naskar, S.C. Kundu, The promotion of osseointegration of titanium surfaces by coating with silk protein sericin, Biomaterials 34 (2013) 2855–2864, https://doi.org/10.1016/j.biomaterials.2013.01.019.
[9] G. Griffanti, W. Jiang, S.N. Nazhat, Bioinspired mineralization of a functionalized injectable dense collagen hydrogel through silk sericin incorporation, Biomater. Sci. 7 (2019) 1064–1077, https://doi.org/10.1039/c8bm01060a.
[10] T. Siritientong, W. Bonani, A. Motta, C. Migliaresi, P. Aramwit, The effects of Bombyx mori silk strain and extraction time on the molecular and biological characteristics of sericin, Biosci. Biotechnol. Biochem. 80 (2016) 241–249, https://doi.org/10.1080/09168451.2015.1088375.
[11] T. Siritientong, T. Srichana, P. Aramwit, The effect of sterilization methods on the physical properties of silk sericin scaffolds, AAPS PharmSciTech 12 (2011) 771–781, https://doi.org/10.1208/s12249-011-9641-y.
[12] H. Kweon, Y.-Y. Jo, H. Seok, S.-G. Kim, W.-S. Chae, S. Sapru, et al., In vivo bone regeneration ability of different layers of natural silk cocoon processed using an eco-friendly method, Macromol. Res. 25 (2017) 806–816, https://doi.org/10.1007/s13233-017-5085-x.
[13] B.B. Mandal, A.S. Priya, S.C. Kundu, Novel silk sericin/gelatin 3-D scaffolds and 2-D films: fabrication and characterization for potential tissue engineering applications, Acta Biomater. 5 (2009) 3007–3020, https://doi.org/10.1016/j.actbio.2009.03.026.
[14] Y. Zhang, P. Zhao, Z. Dong, D. Wang, P. Guo, X. Guo, et al., Comparative proteome analysis of multi-layer cocoon of the silkworm, Bombyx mori, PLoS One 10 (2015), e0123403, https://doi.org/10.1371/journal.pone.0123403.
[15] Y.-J. Kang, Y.-Y. Jo, H. Kweon, W.-S. Chae, W.-G. Yang, U. Garagiola, et al., Comparison of the physical properties and in vivo bioactivities of flatwise-spun silk mats and cocoon-derived silk mats for guided bone regeneration, Macromol. Res. 28 (2020) 159–164, https://doi.org/10.1007/s13233-020-8026-z.
[16] Y.-Y. Jo, H. Kweon, D.-W. Kim, K. Baek, M.-K. Kim, S.-G. Kim, et al., Bone regeneration is associated with the concentration of tumour necrosis factor-a induced by sericin released from a silk mat, Sci. Rep. 7 (2017) 15589, https://doi.org/10.1038/s41598-017-15687-w.
[17] J.-W. Kim, Y.-Y. Jo, J.-Y. Kim, J.-H. Oh, B.-E. Yang, S.-G. Kim, Clinical study for silk mat application into extraction socket: a Split-mouth, randomized clinical trial, Appl. Sci. 9 (2019) 1208, https://doi.org/10.3390/app9061208.
[18] J.W. Kim, Y.Y. Jo, H.Y. Kweon, D.W. Kim, S.G. Kim, The effects of proteins released from silk mat layers on macrophages, Maxillofac. Plast. Reconstr. Surg. 40 (2018) 10, https://doi.org/10.1186/s40902-018-0149-1.
[19] G.S. Anusuya, M. Kandasamy, S.A.Jacob Raja, S. Sabarinathan, P. Ravishankar, B. Kandhasamy, Bone morphogenetic proteins: signaling periodontal bone regeneration and repair, J. Pharm. Bioallied Sci. 8 (2016), S39-S41, https://doi.org/10.4103/0975-7406.191964.
[20] M.A. Valdes, N.A. Thakur, S. Namdari, D.M. Ciombor, M. Palumbo, Recombinant bone morphogenic protein-2 in orthopaedic surgery: a review, Arch. Orthop. Trauma Surg. 129 (2009) 1651–1657, https://doi.org/10.1007/s00402-009-0850-8.
[21] D. Bowler, H. Dym, Bone morphogenic protein: application in implant dentistry, Dent. Clin. N. Am. 59 (2015) 493–503, https://doi.org/10.1016/j.cden.2014.10.006.
[22] A. Young, A. Mirarchi, Soft tissue swelling associated with the use of recombinant human bone morphogenetic protein-2 in long bone non-unions, J. Orthop. Case Rep. 5 (2015) 18–21.
[23] K.W. Zaid, M. Chantiri, G. Bassit, Recombinant human bone morphogenetic Protein-2 in development and progression of Oral squamous cell carcinoma, Asian Pac. J. Cancer Prev. 17 (2016) 927–932, https://doi.org/10.7314/apjcp.2016.17.3.927.
[24] E.J. Carragee, E.L. Hurwitz, B.K. Weiner, A critical review of recombinant human bone morphogenetic protein-2 trials in spinal surgery: emerging safety concerns and lessons learned, Spine J. 11 (2011) 471–491, https://doi.org/10.1016/j.spinee.2011.04.023.
[25] K.B. Lee, C.E. Taghavi, S.S. Murray, K.J. Song, G. Keorochana, J.C. Wang, BMP induced inflammation: a comparison of rhBMP-7 and rhBMP-2, J. Orthop. Res. 30 (2012) 1985–1994, https://doi.org/10.1002/jor.22160.
[26] D.B. Raina, D. Larsson, F. Mrkonjic, H. Isaksson, A. Kumar, L. Lidgren, et al., Gelatin- hydroxyapatite- calcium sulphate based biomaterial for long term sustained delivery of bone morphogenic protein-2 and zoledronic acid for increased bone formation: in-vitro and in-vivo carrier properties, J. Control. Release 272 (2018) 83–96, https://doi.org/10.1016/j.jconrel.2018.01.006.
[27] Z.J. Li, C.T. Lu, R.F. Lai, Ectopic osteogenesis effect of antigen-extracted xenogeneic cancellous bone graft with chitosan/rhBMP-2/bFGF sequential sustained-release nanocapsules, J. Biomater. Appl. 33 (2018) 23–43, https://doi.org/10.1177/0885328218761193.

[28] J. Gobom, E. Nordhoff, E. Mirgorodskaya, R. Ekman, P. Roepstorff, Sample purification and preparation technique based on nano-scale reversed-phase columns for the sensitive analysis of complex peptide mixtures by matrix-assisted laser desorption/ionization mass spectrometry, J. Mass Spectrom. 34 (1999) 105–116, https://doi.org/10.1002/(SICI)1096-9888(199902)34:2<105::AID-JMS768>3.0.CO;2-4.
[29] K. Baek, D. Park, H.R. Hwang, S.-G. Kim, H. Lee, J.-H. Baek, Blocking ß1/ß2-adrenergic signaling reduces dietary fat absorption by suppressing expression of pancreatic lipase in high fat-fed mice, Int. J. Mol. Sci. 19 (2018) 857, https://doi.org/10.3390/ijms19030857.
[30] J. Kong, S. Yu, Fourier transform infrared spectroscopic analysis of protein secondary structures, Acta Biochim. Biophys. Sin. 39 (2007) 549–559, https://doi.org/10.1111/j.1745-7270.2007.00320.x.
[31] A. Takeuchi, C. Ohtsuki, T. Miyazaki, M. Kamitakahara, S. Ogata, M. Yamazaki, et al., Heterogeneous nucleation of hydroxyapatite on protein: structural effect of silk sericin, J. R. Soc. Interface 2 (2005) 373–378, https://doi.org/10.1098/rsif.2005.0052.
[32] A. Garel, G. Deleage, J.C. Prudhomme, Structure and organization of the Bombyx mori sericin 1 gene and of the sericins 1 deduced from the sequence of the ser 1B cDNA, Insect Biochem. Mol. Biol. 27 (1997) 469–477, https://doi.org/10.1016/s0965-1748(97)00022-2.
[33] P. Aramwit, A. Sangcakul, The effects of sericin cream on wound healing in rats, Biosci. Biotechnol. Biochem. 71 (2007) 2473–2477, https://doi.org/10.1271/bbb.70243.
[34] S. Nayak, T. Dey, D. Naskar, S.C. Kundu, The promotion of osseointegration of titanium surfaces by coating with silk protein sericin, Biomaterials 34 (12) (2013) 2855–2864, https://doi.org/10.1016/j.biomaterials.2013.01.019.
[35] M. Yang, G. Zhou, Y. Shuai, J. Wang, L. Zhu, C. Mao, Ca(2)-induced self-assembly of Bombyx mori silk sericin into a nanofibrous network-like protein matrix for directing controlled nucleation of hydroxylapatite nano-needles, J. Mater. Chem. B 3 (12) (2015) 2455–2462, https://doi.org/10.1039/C4TB01944J.
[36] M. Yang, Y. Shuai, C. Zhang, Y. Chen, L. Zhu, C. Mao, et al., Biomimetic nucleation of hydroxyapatite crystals mediated by Antheraea pernyi silk sericin promotes osteogenic differentiation of human bone marrow derived mesenchymal stem cells, Biomacromolecules 15 (2014) 1185–1193, https://doi.org/10.1021/bm401740x.
[37] S.-G. Kim, H. Kweon, Y.-Y. Jo, Toll-like receptor and silk sericin for tissue engineering, Int. J. Indust. Entomol. 42 (2021) 1–6, https://doi.org/10.7852/ijie.2021.42.1.1.
[38] L.A. O'Neill, D. Golenbock, A.G. Bowie, The history of toll-like receptors - redefining innate immunity, Nat. Rev. Immunol. 13 (2013) 453–460, https://doi.org/10.1038/nri3446.
[39] H.S. Kulkarni, D. Scozzi, A.E. Gelman, Recent advances into the role of pattern recognition receptors in transplantation, Cell. Immunol. 351 (2020), 104088, https://doi.org/10.1016/j.cellimm.2020.104088.
[40] N. Coté, A. Mahmut, Y. Bosse, C. Couture, S. Pagé, S. Trahan, et al., Inflammation is associated with the remodeling of calcific aortic valve disease, Inflammation 36 (2013) 573–581, https://doi.org/10.1007/s10753-012-9579-6.
[41] J. Park, H. Myoung, Chronic suppurative osteomyelitis with proliferative periostitis related to a fully impacted third molar germ: a report of two cases, J. Korean Assoc. Oral Maxillofac. Surg. 42 (2016) 215–220, https://doi.org/10.5125/jkaoms.2016.42.4.215.
[42] D. Vlachakis, S.C. Tsaniras, C. Feidakis, S. Kossida, Molecular modelling study of the 3D structure of the biglycan core protein, using homology modelling techniques, J. Mol. Biochem. 2 (2013) 85–93.
[43] A. Babelova, K. Moreth, W. Tsalastra-Greul, J. Zeng-Brouwers, O. Eickelberg, M. F. Young, et al., Biglycan, a danger signal that activates the NLRP3 inflammasome via toll-like and P2X receptors, J. Biol. Chem. 284 (2009) 24035–24048, https://doi.org/10.1074/jbc.M109.014266.
[44] L. Schaefer, A. Babelova, E. Kiss, H.-J. Hausser, M. Baliova, M. Krzyzankova, et al., The matrix component biglycan is proinflammatory and signals through toll-like receptors 4 and 2 in macrophages, J. Clin. Invest. 115 (2005) 2223–2233, https://doi.org/10.1172/JCI23755.
[45] R. Song, D.A. Fullerton, L. Ao, D. Zheng, K.-S. Zhao, X. Meng, BMP-2 and TGF-ß1 mediate biglycan-induced pro-osteogenic reprogramming in aortic valve interstitial cells, J. Mol. Med. (Berl) 93 (2015) 403–412, https://doi.org/10.1007/s00109-014-1229-z.
[46] X. Su, L. Ao, Y. Shi, T.R. Johnson, D.A. Fullerton, X. Meng, Oxidized low density lipoprotein induces bone morphogenetic protein-2 in coronary artery endothelial cells via toll-like receptors 2 and 4, J. Biol. Chem. 286 (2011) 12213–12220, https://doi.org/10.1074/jbc.M110.214619.
[47] R. Chehin, D. Rengel, J.C. Milicua, F.M. Goni, J.L. Arrondo, G. Pifat, Early stages of LDL oxidation: apolipoprotein B structural changes monitored by infrared spectroscopy, J. Lipid Res. 42 (2001) 778–782, https://doi.org/10.1016/S0022-2275(20)31640-0.
[48] X. Yang, D.A. Fullerton, X. Su, L. Ao, J.C. Cleveland, X. Meng, Pro-osteogenic phenotype of human aortic valve interstitial cells is associated with higher levels of toll-like receptors 2 and 4 and enhanced expression of bone morphogenetic protein 2, J. Am. Coll. Cardiol. 53 (2009) 491–500.
[49] Q. Zhan, R. Song, Q. Zeng, Q. Yao, L. Ao, D. Xu, et al., Activation of TLR3 induces osteogenic responses in human aortic valve interstitial cells through the NF-kappaB and ERK1/2 pathways, Int. J. Biol. Sci. 11 (2015) 482–493, https://doi.org/10.7150/ijbs.10905.
[50] Y. Nomura, C. Fukui, Y. Morishita, Y. Haishima, A biological study establishing the endotoxin limit for osteoblast and adipocyte differentiation of human mesenchymal stem cells, Regen. Ther. 8 (2018) 46–57, https://doi.org/10.1016/j.reth.2018.01.002.
[51] Z. Pang, R.D. Junkins, R. Raudonis, A.J. MacNeil, C. McCormick, Z. Cheng, et al., Regulator of calcineurin 1 differentially regulates TLR-dependent MyD88 and TRIF signaling pathways, PLoS One 13 (2018), e0197491, https://doi.org/10.1371/journal.pone.0197491.
[52] S. Al-Halifa, X. Zottig, M. Babych, M. Côté-Cyr, S. Bourgault, D. Archambault, Harnessing the activation of toll-like receptor 2/6 by self-assembled cross-ß fibrils to design adjuvanted nanovaccines, Nanomaterials (Basel) 10 (2020) 1981, https://doi.org/10.3390/nano10101981.
[53] C. Tukel, R.P. Wilson, J.H. Nishimori, M. Pezeshki, B.A. Chromy, A.J. Baumler, Responses to amyloids of microbial and host origin are mediated through toll-like receptor 2, Cell Host Microbe 6 (2009) 45–53, https://doi.org/10.1016/j.chom.2009.05.020.
[54] Z. Chen, T. Klein, R.Z. Murray, R. Crawford, J. Chang, C. Wu, et al., Osteoimmunomodulation for the development of advanced bone biomaterials, Mater. Today (Kidlington) 19 (2016) 304–321, https://doi.org/10.1016/j.mattod.2015.11.004.
[55] S.G. Kim, Immunomodulation for maxillofacial reconstructive surgery, Maxillofac. Plast. Reconstr. Surg. 42 (2020) 5, https://doi.org/10.1186/s40902-020-00249-4.
[56] P.R. Dube, L. Birnbaumer, G. Vazquez, Evidence for constitutive bone morphogenetic protein-2 secretion by M1 macrophages: constitutive auto/paracrine osteogenic signaling by BMP-2 in M1 macrophages, Biochem. Biophys. Res. Commun. 491 (2017) 154–158, https://doi.org/10.1016/j.bbrc.2017.07.065.
[57] A. Kurioka, F. Kurioka, M. Yamazaki, Characterization of sericin powder prepared from citric acid-degraded sericin polypeptides of the silkworm, bombyx Mori, Biosci. Biotechnol. Biochem. 68 (2004) 774–780, https://doi.org/10.1271/bbb.68.774.
[58] H. Yun, M.K. Kim, H.W. Kwak, J.Y. Lee, M.H. Kim, K.H. Lee, The role of glycerol and water in flexible silk sericin film, Int. J. Biol. Macromol. 82 (2016) 945–951, https://doi.org/10.1016/j.ijbiomac.2015.11.016.
[59] R.S. Graham, B.J. Samsell, A. Proffer, M.A. Moore, R.A. Vega, J.M. Stary, et al., Evaluation of glycerol-preserved bone allografts in cervical spine fusion: a prospective, randomized controlled trial, J. Neurosurg. Spine 22 (2015) 1–10, https://doi.org/10.3171/2014.9.SPINE131005.